

# Parametric and Adsorption Kinetic Studies of Methylene Blue Removal from Textile Simulated Wastewater using Oil Palm EFB

S. M. Anisuzzaman<sup>1</sup>, Collin G. Joseph<sup>2,\*</sup>, Nur H. Mustafa<sup>2</sup>, Sabrina Soloi<sup>2</sup>

<sup>1</sup>Chemical Engineering Programme, Faculty of Engineering, Universiti Malaysia Sabah  
88400 Kota Kinabalu, Sabah, Malaysia

<sup>2</sup>Industrial Chemistry Programme, Faculty of Science and Natural Resources  
Universiti Malaysia Sabah, 88400 Kota Kinabalu, Sabah, Malaysia

\*Corresponding author (e-mail: collin@ums.edu.my)

In this study, the removal of methylene blue (MB) dye from water samples by adsorption onto oil palm empty fruit bunches (EFB) was explored. The adsorption experiments were carried out at different initial dye concentrations (2 - 10 mg/L), solution pH levels (3 - 11), contact times (60 min), and biosorbent dosages (0.3 - 0.7 g). MB removal was found to increase with a lower initial dye concentration, higher biosorbent dosage and increased contact time. The removal rate was rapid for the first 20 min, and reached equilibrium at 60 min. Adsorption was favourable at a pH above 11. Langmuir and Freundlich adsorption isotherm models as well as pseudo-first order and pseudo-second order kinetic models were considered in order to understand the adsorption mechanisms. The equilibrium data was best represented by the Freundlich isotherm model which had a high  $R^2$  value of 0.9761. The Freundlich model represented a heterogenous EFB surface with a multilayer adsorption pattern which was supported by the adsorption constant,  $n$  which had a value of 1.0366 that satisfied the heterogeneity requirement. The kinetic rates complied with a pseudo-second order model indicating that chemisorption controlled the adsorption process. In this study, the EFB surface was characterized using Fourier transform infrared spectroscopy (FTIR) and Brunauer, Emmett and Teller (BET) analysis. The results suggest that EFB would be an excellent alternative low-cost biosorbent for the removal of cationic dyes from textile industry effluent.

**Keywords:** EFB; methylene blue; biosorbent; adsorption; sorption isotherm

Received: January 2023; Accepted: March 2023

Contamination of water resources due to industrial effluents is an unavoidable problem in developing countries. This phenomenon causes 70 - 80% of all illnesses in these countries and is related to water contamination [1]. The main sources of water contamination are industrialization, civilization, agricultural activities, and other environmental changes [2]. Examples of some contaminants present in wastewater include dyes, heavy metals and organic pollutants [3,4]. Most dyes are resistant to environmental conditions such as heat, photodegradation and biodegradation due to their complex aromatic structures which indirectly provide them physicochemical, thermal and optical stability [5,6]. Methylene blue (MB) is a thiazine dye that is used as a redox indicator in chemistry, for bacterial staining, and to determine yeast cell viability in the field of biology, as well as acting as a dyestuff for cotton, wool, paper and silk [6]. There are many physical and chemical techniques that are usually used for removing dyes from industrial effluent, such as chemical flocculation, electro-flotation, precipitation, electro-kinetic coagulation, ion exchange, membrane filtration, electrochemical destruction, irradiation, ozonation, chemical oxidation, reverse osmosis, ultra-filtration [6], photodegradation and anaerobic treatment [3-8]. However, these techniques

possess several limitations such as high cost, requirement of activating agents and generation of sludge. Biological treatments are advantageous in the removal of suspended solids, but are not helpful for removing dye compounds from wastewater. Adsorption by activated carbon (AC) was found to be superior compared to other techniques for the removal of dyes from aqueous solutions [8-12]. However, AC is not used commercially due to its high cost of manufacturing and regeneration of the spent carbon [9-10].

Many low-cost adsorbents for dyes and metals have been investigated. These low-cost adsorbents such as jute stick powder, cattail roots, peanut hulls, orange peels, coir pith, hardwood sawdust, bagasse pith, soy meal husks, rice husks, maize stalks, hazelnut shells, bottom ash, papaya seeds, guava (*psidiumguajava*) leaf powder, wheat bran, jackfruit peels etc. are sourced from agricultural waste and have proven effective in the removal of dyes from wastewater [10-15]. In this study, oil palm empty fruit bunches (EFB) were chosen as a biosorbent due to the abundance of this agricultural waste material. As mentioned by Shaiful *et al.* [15], this biosorbent does not require any expensive additional pre-treatment steps. Moreover, biosorption is a novel approach, competitive, effective and cheap

compared to other types of adsorbents [16-18]. Thus, EFB was used without complex and costly pre-treatment steps or an activation process for wastewater remediation. The effectiveness of EFB as an MB biosorbent in aqueous solutions was evaluated using parametric variables such as dye concentration, contact time, pH and biosorbent dosage. The equilibrium and kinetic data were analysed to study the biosorption isotherm and kinetics of EFB. Characterization of the EFB surface was also carried out.

## MATERIALS AND METHODOLOGY

### Adsorbate

MB ( $C_{16}H_{18}ClN_3S \cdot 3H_2O$ ) was obtained from Aldrich and used as an adsorbate without further purification. A stock solution was prepared by dissolving 1.0 g of MB in 1000 mL of distilled water in a volumetric flask. This stock solution was kept in a reagent bottle for future use.

### Preparation and Characterization of Biosorbent

A sample of EFB was washed several times with distilled water to remove any dirt, and subsequently dried in an oven at 110 °C for 48 h. The dried EFB was cut and sieved to a size of 0.2 mm. Finally, the resulting product was stored in an air-tight container for further use. No further chemical or physical treatments were performed on the biosorbent. The surface chemistry of the powdered EFB sample was analysed using Fourier Transform infrared spectroscopy (FTIR) (Perkin Elmer, Spectrum 100, USA) to determine the surface functional groups. Surface properties such as specific surface area, pore size distribution and total pore volume were analysed using the Brunauer-Emmett-Teller (BET) method. The absorbance of MB was measured using a UV-Vis spectrometer (Perkin Elmer, Lambda 25). In this method, distilled water was used as the blank solution. The measurements were made in triplicate to obtain an accurate calibration. The absorbance values obtained were used to plot a calibration curve of absorbance versus concentration.

### BET Analysis

The BET surface area and pore size distribution were determined from the nitrogen isotherm at 77.3 K using a Quantachrome Autosorb automated gas sorption instrument.

### Effect of Initial Dye Concentration

In order to study the effect of the initial dye concentration on the adsorption uptake, 200 mL MB solutions with initial concentrations  $C_i$ , of 2 mg/L, 4

mg/L, 6 mg/L, 8 mg/L and 10 mg/L were prepared in a series of 250 mL Erlenmeyer flasks. These solutions were analysed by measuring their absorbance values at 664 nm using ultraviolet-visible (UV-Vis) spectroscopy. Then, 0.1 g of the EFB biosorbent was added into each Erlenmeyer flask and the flasks were placed in an orbital shaker at room temperature. The mixtures were stirred at a constant speed of 150 rpm until equilibrium was reached. The final dye concentration,  $C_e$  was measured and the amount of dye adsorbed,  $q_t$  (mg/g) was calculated according to equation 1 [19]:

$$q_t = (C_0 - C_e) \frac{V}{W} \quad (1)$$

where  $C_0$  (mg/L) is the initial concentration and  $C_e$  (mg/L) is the final concentration of the MB, whereas  $V$  is the volume of the dye solution (L) and  $W$  is the mass of the adsorbent used (g).

### Effect of Biosorbent Dosage

The effect of biosorbent dosage on the adsorption process was studied by varying the mass of EFB (3 g, 5 g and 7 g) in an MB solution of constant volume (200 mL), and concentration (4 mg/L). The different dosages of EFB were individually added to three different flasks and mixed using a shaker for 25 min. The residual concentration of MB in the filtrate was measured and its adsorption capacity (mg/g) was calculated as the mass of MB adsorbed onto EFB divided by the amount of EFB added to the flask. The percentage of dye removal was calculated according to the equation below,

$$\% \text{ Dye removal} = \frac{C_0 - C_e}{C_0} \times 100\% \quad (2)$$

### Effect of Solution pH

The effect of solution pH on the adsorption process was studied at pH 3, 7 and 11. The pH was adjusted using 0.1 M HCl and 0.1 M NaOH. The initial dye concentration ( $C_0$ ) was fixed at 4 mg/L with a biosorbent dosage of 1.0 g while the solution was kept at room temperature. The final dye concentration ( $C_e$ ) was measured and the percentage removal of dye was calculated using equation (2).

### Effect of Time

Adsorption kinetics experiments were performed by contacting a 200 mL solution of MB with different initial concentrations (2 mg/L, 4 mg/L, 6 mg/L, 8 mg/L and 10 mg/L) with 1.0 g of EFB powder in a 250 mL Erlenmeyer flask at room temperature. The extracted samples were injected into sample vials for storage before analysis.

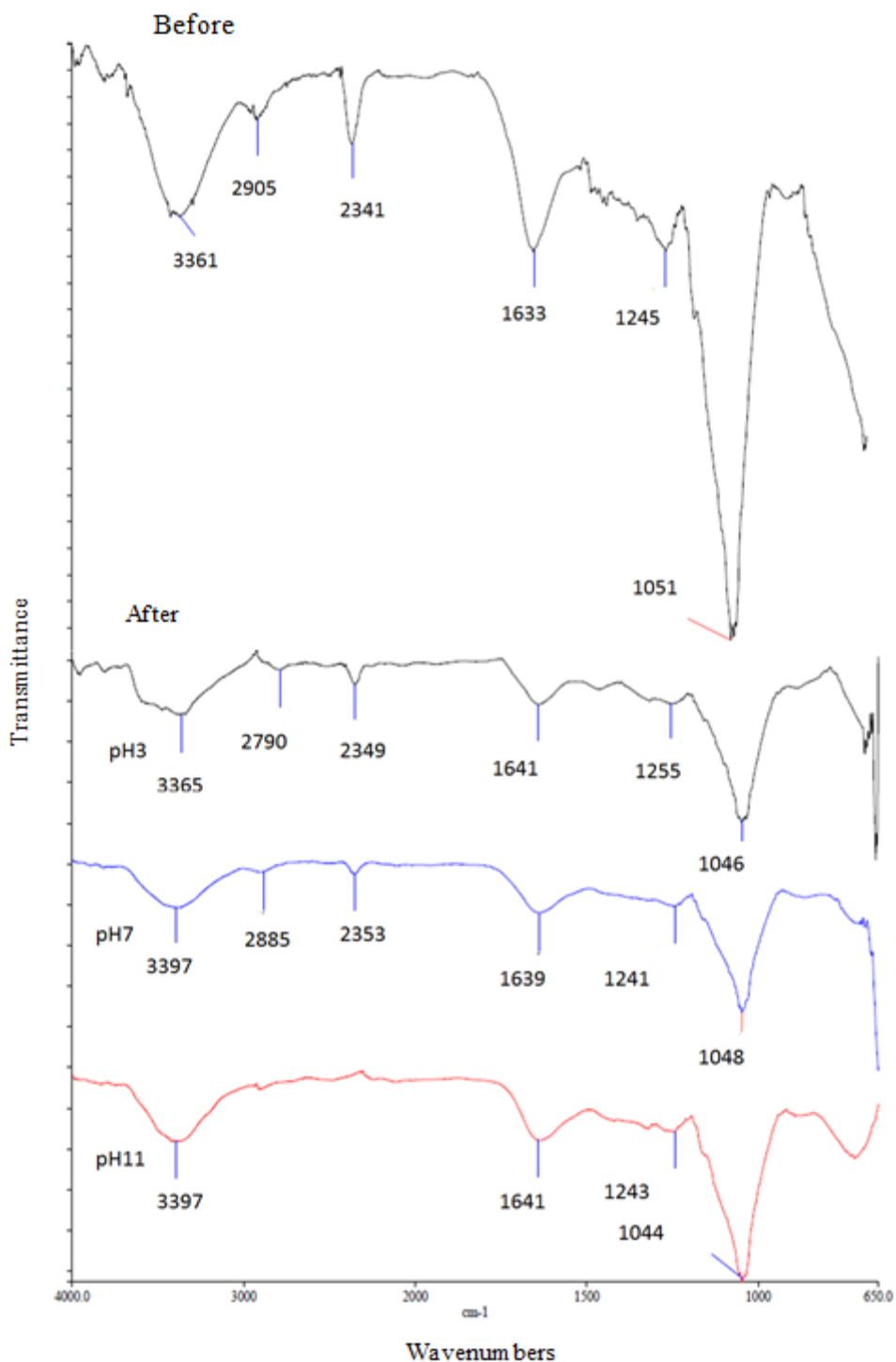


**Figure 1.** FTIR spectra of EFB before and after adsorption at different pH.

## RESULTS AND DISCUSSION

### Surface Chemistry Studies of EFB

Figure 1 shows the FTIR spectra of EFB before and after adsorption at different pH values. These indicate that various functional groups were present on the surface of the EFB sample. By comparing the spectra of EFB before and after adsorption, it is clear that some peaks had shifted, while some disappeared after

undergoing adsorption. Before the adsorption process, the O-H stretching mode of EFB was observed in the region of  $3300\text{ cm}^{-1}$ , while peaks at  $2905\text{ cm}^{-1}$  were related to the C-H vibration of the  $\text{CH}_3$  and  $\text{CH}_2$  groups present in the EFB. The peak at  $1051\text{ cm}^{-1}$  represents C-O stretching of cellulose, hemi-cellulose and lignin in the EFB. The wavelength around  $1633\text{ cm}^{-1}$  was due to the aromatic lignin. The peak at  $2341\text{ cm}^{-1}$  was assigned to the  $\text{C}\equiv\text{C}$  stretching while that at  $1245\text{ cm}^{-1}$  was due to C-N stretching. In the FTIR graph of EFB

after adsorption, the peak that was at  $3361\text{ cm}^{-1}$  before adsorption shifted to  $3365\text{ cm}^{-1}$  after adsorption at pH 3, and  $3397\text{ cm}^{-1}$  at pH 7 and pH 11. This shift when the pH was increased may be due to the concentration of  $\text{OH}^-$  that increased after adsorption. For the C-H vibration at  $2905\text{ cm}^{-1}$ , there was a shift after adsorption at every pH to  $2790\text{ cm}^{-1}$  and  $2885\text{ cm}^{-1}$  with increasing solution pH until it disappeared at pH 11. Figure 1 also shows that there was a shift of the  $\text{C}\equiv\text{C}$  stretching peak from  $2341\text{ cm}^{-1}$  before adsorption to  $2349\text{ cm}^{-1}$  at pH 3,  $2353\text{ cm}^{-1}$  at pH 7, while it went missing at pH 11 due to surface interactions between EFB and MB. After adsorption at pH 3, pH 7 and pH 11, the aromatic lignin at  $1633\text{ cm}^{-1}$  shifted to  $1641\text{ cm}^{-1}$ ,  $1639\text{ cm}^{-1}$ , and  $1641\text{ cm}^{-1}$ , respectively, due to the presence of the aromatic rings in MB. The peak at  $1245\text{ cm}^{-1}$  that represents C-N stretching was detected at  $1255\text{ cm}^{-1}$  at pH 3, indicating C-H wagging. This may be due to the high concentration of positively charged ions being replaced by negatively charged nitrogen ions. However, at pH 7 and pH 11, there was

no C-H wagging, but the peak shifted to  $1241\text{ cm}^{-1}$  and  $1243\text{ cm}^{-1}$  respectively, indicating functional group interactions. The peak at  $1051\text{ cm}^{-1}$  which represents C-O stretching also showed a slight shift to  $1046\text{ cm}^{-1}$ ,  $1048\text{ cm}^{-1}$ , and  $1044\text{ cm}^{-1}$  respectively.

### Surface Area and Pore-distribution

Table 1 lists the values for the total surface area, total pore volume, average pore diameter and Langmuir surface area of the EFB sample. The BET surface area and Langmuir surface area were found to be  $2.179\text{ m}^2/\text{g}$  and  $5.072\text{ m}^2/\text{g}$ , respectively, using the nitrogen adsorption isotherm method. From nitrogen adsorption isotherm analysis, it was found that the isotherm of EFB, as defined by the International Union of Pure and Applied Chemistry (IUPAC) classification, was a type III isotherm. The average pore diameter of EFB was  $275.7\text{ \AA}$ , suggesting that it was a mesoporous material. Hence, it should be suitable for adsorption processes.

**Table 1.** Surface characteristics of EFB.

Surface characteristics	Values
Total surface area ( $S_{\text{BET}}$ )	$2.179\text{ m}^2/\text{g}$
Total pore volume ( $V_{\text{T}}$ )	$0.01502\text{ cc/g}$
Average pore diameter ( $d_{\text{av}}$ )	$275.7\text{ \AA}$
Langmuir surface area	$5.072\text{ m}^2/\text{g}$

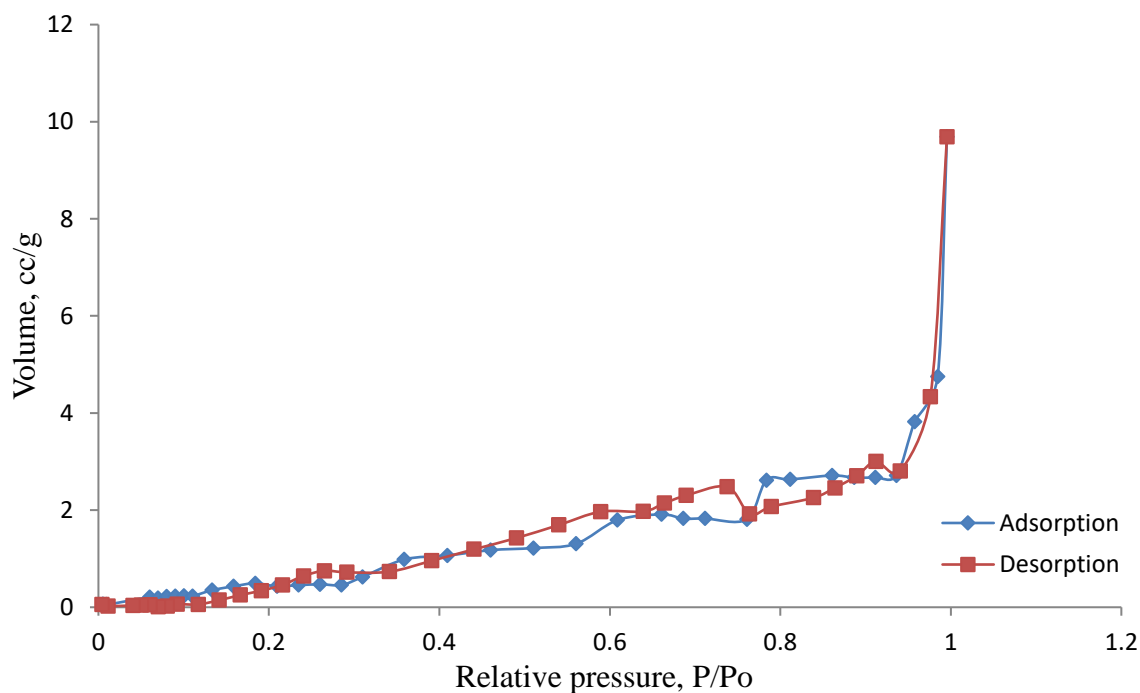


**Figure 2.** Nitrogen adsorption isotherm of EFB.

Figure 2 shows the nitrogen adsorption-desorption isotherm of EFB. The beginning of the hysteresis loop was very close to zero relative pressure, indicating that the inability to dry the sample at this point may account for the lack of reproducibility of the adsorption. The hysteresis phenomenon has been observed in nitrogen adsorption-desorption measurements. According to Aligizaki [20], the Type III isotherm shows no rapid initial uptake of gas, and occurs when the interaction between adsorbent and adsorbate is rather weak. This is seen with non-porous solids or solids with macropores, and is indicative of a small surface area.

**Effect of Initial Concentration and Contact Time**

To investigate the effect of initial dye concentration, different concentrations (2 - 10 mg/L) were used. Table 2 shows the percentage removal of MB was above 92 % for a contact time of 60 min. However, the adsorption capacity increased with initial concentration from 3.70 mg/L at 2 mg/L initial concentration to 18.40 mg/L at a concentration of 10 mg/L. According

to Haris and Sathasivan [21], this phenomenon occurred because the interactions between the adsorbent surface and the dye molecules increased due to a higher number of dye molecules colliding with the adsorbent when the initial concentration was high. This resulted in an increase in adsorption capacity. However, the percentage removal was reduced due to the saturation effect of the dye on the adsorbent surface.

Figure 3 indicates how the percentage removal of MB increased rapidly with time, while Figure 4 shows the rapid decrease in dye concentration with time. Both graphs show that the rate slowed after a period of time. This is because the longer contact time pushed the reaction towards equilibrium. From Figure 3, the removal rate of MB rapidly increased during the first 20 min of contact time, and equilibrium was achieved after 60 min of contact. This phenomenon was due to large numbers of free surface sites available for adsorption during the initial stage, but after a certain amount of time, the surface becomes saturated [22]. The colour removal efficiency of EFB at 60 min was a high 92.87 % with a 2 mg/L initial dye concentration.

**Table 2.** Table of percentage removal and adsorption capacity of MB at 60 min for different initial concentrations.

Initial concentration (mg/L)	Percentage removal (%)	Adsorption capacity (mg/L)
2	92.87	3.70
4	92.82	7.43
6	92.41	11.09
8	92.45	14.79
10	92.04	18.40

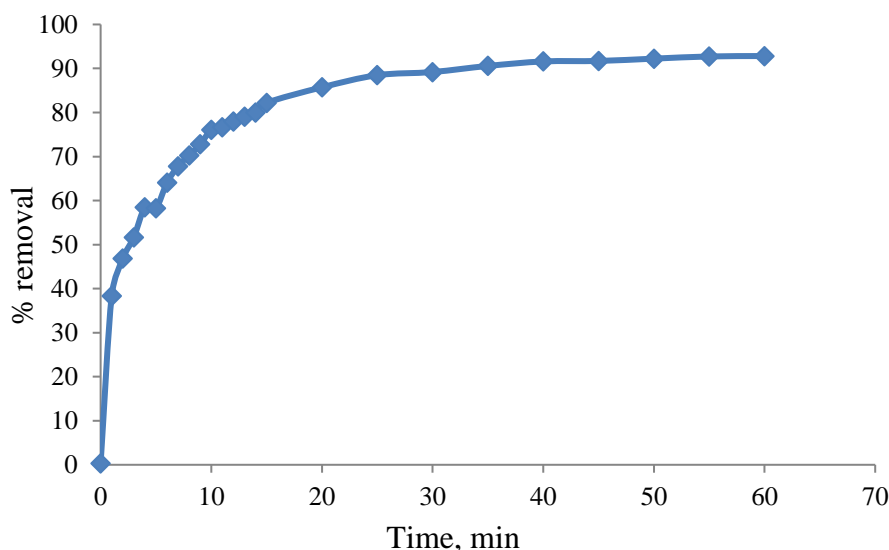


**Figure 3.** Percentage removal of MB against time with 4 mg/L initial concentration.

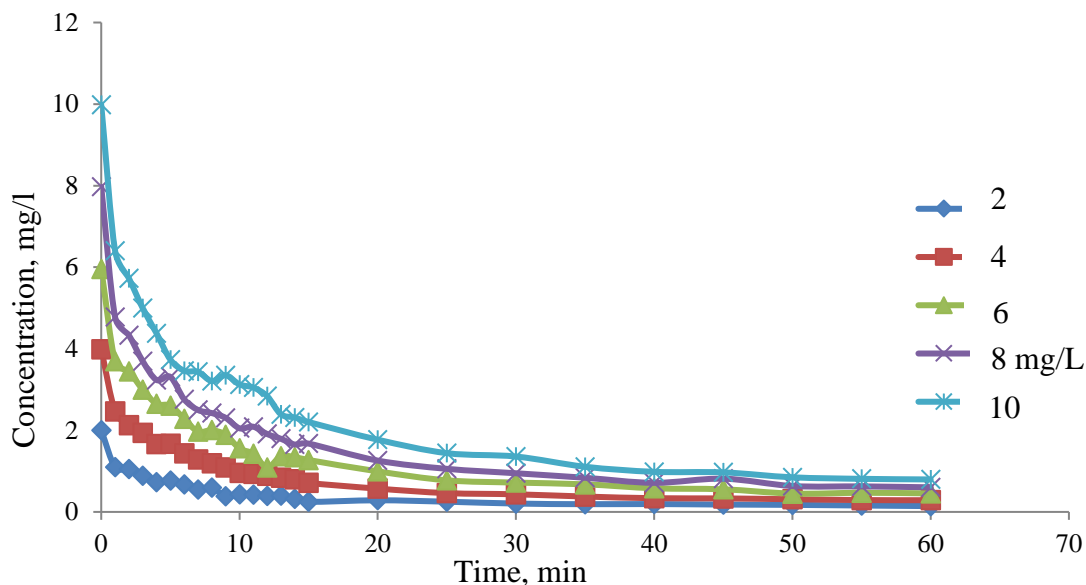


Figure 4. MB concentration against time at different initial concentrations.

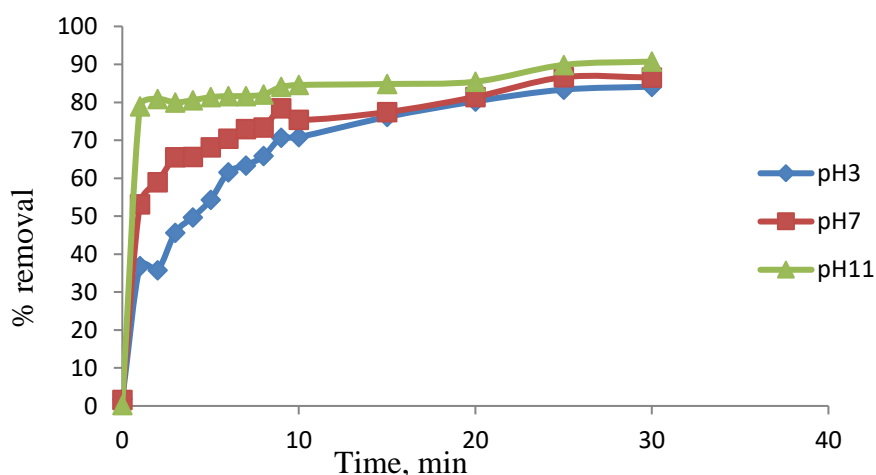


Figure 5. Percentage removal of MB against time at different pH.

### Effect of pH

Figure 5 shows the percentage removal of MB against time at different pH levels. It is clear that the removal rate increased with pH. The highest percentage removal of MB of 90.74 % was obtained at pH 11, followed by pH 7, and pH 3 with 86.53 % and 84.12 % respectively.

At pH 11, the solution had an increased  $\text{OH}^-$  ion concentration while the surface of EFB acquired

a negative charge by absorbing  $\text{OH}^-$  ions. When the surface of EFB is negatively charged, it forms a strong electrostatic attraction with the cationic dye, MB. This leads to a high adsorption of the dye [23]. However, when the pH is lower, the number of positively charged  $\text{H}^+$  ions on the EFB surface increases, which does not favour the adsorption of cationic dyes; instead, it will cause electrostatic repulsion. In addition, the lower adsorption of the dye in acidic conditions is due to the competition between the many  $\text{H}^+$  ions and the MB dye molecules for the adsorption sites [24].

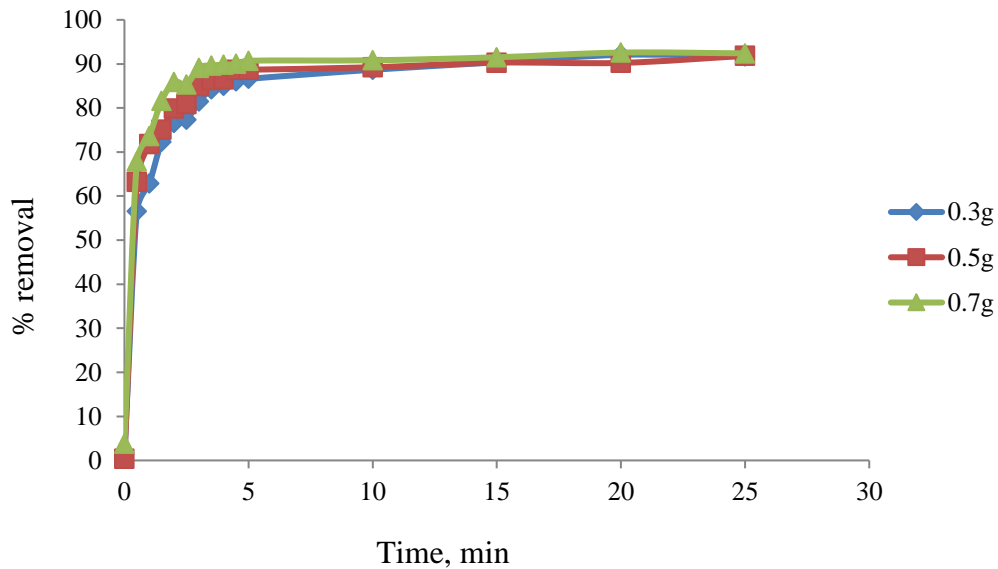


**Figure 6.** Percentage removal of MB against time at different dosages of EFB.

### Effect of Biosorbent Dosage

The adsorption of MB dye was studied with different dosages of EFB (0.3 g, 0.5 g, and 0.7 g) in a constant volume of 200 mL agitated for 30 min at 150 rpm in an orbital shaker. The dosage of adsorbent is a key parameter that controls both the availability and accessibility of the adsorption site [25]. Figure 6 shows the percentage removal of MB against time at different dosages of EFB. From Figure 6, the percentage removal of MB increased with biosorbent dosage, with 0.5 g giving the highest percentage removal of MB at 91.82 %. Fixed dosages of EFB only absorb a certain amount of dye. When a small amount of EFB is present, only a small amount of MB can be adsorbed, while a higher dosage contains more adsorption sites [26]. Thus, a higher dosage of EFB will remove a higher percentage of dye and have a larger adsorption capacity.

### Adsorption Isotherm Studies

The Langmuir and Freundlich equations were used to study the interactions between the EFB biosorbent and MB dye. The Langmuir isotherm was used to

determine the adsorption capacity,  $Q_o$ . The Langmuir constant,  $K_L$ , was involved in the rate of adsorption as follows [27]:

$$\frac{C_e}{q_e} = \frac{1}{Q_o K_L} + \frac{C_e}{Q_o} \quad (3)$$

The Freundlich model assumes heterogeneous surface energies, while the energy of the Langmuir equation varies as a function of surface coverage. The linear form of the Freundlich equation is as follows [28]:

$$\text{Log } q_e = \text{log } K_F + \left(\frac{1}{n}\right) \text{log } C_e \quad (4)$$

According to the Langmuir equation,  $Q_o$  represents the monolayer sorption capacity where a higher value of  $Q_o$  results from a higher surface area and pore volume [24]. The Langmuir adsorption isotherm graph is plotted with  $\frac{C_e}{q_e}$  against  $C_e$  as seen in Figure 7. It forms a linear graph with an  $R^2$  value of 0.1993. As the  $R^2$  value obtained was too small, it could not be used to describe the adsorption pattern. The  $Q_o$  value obtained from this study was 151.5 mg/g.

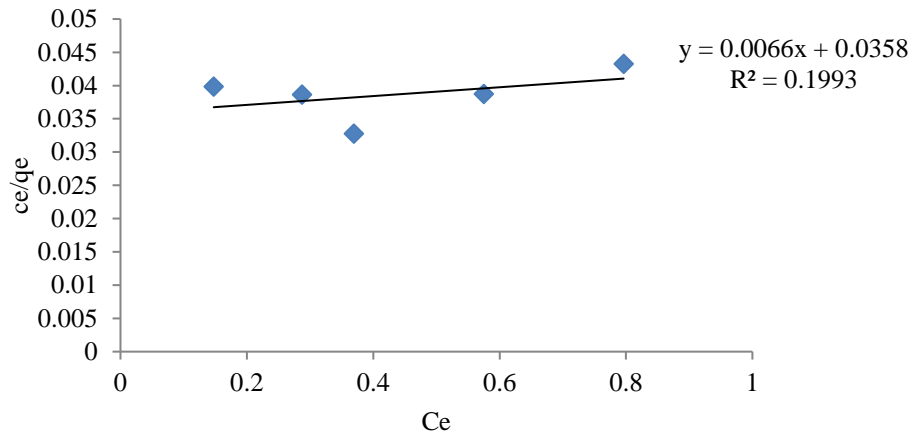


Figure 7. Langmuir isotherm.

In order to describe the adsorption process type and the adsorption affinities between the adsorbate and adsorbent, the dimensionless separation factor  $R_L$  was calculated from Equation 5:

$$R_L = \frac{1}{1 + K_L C_0} \quad (5)$$

In this study, the  $R_L$  value of the Langmuir isotherm was favourable to adsorption since the its calculated value of 0.3517 was between 0 and 1 ( $0 < R_L < 1$ ). Hence, this confirmed that there was good adsorption of MB dye by EFB under the conditions of this study. The analysis of the isotherm data is important to develop an equation which accurately re-

presents the results and can be used for design purposes.

The linear graph of the Freundlich isotherm is given in Figure 8, where  $\log q_e$  is plotted against  $\log C_e$ . The Freundlich isotherm gave a higher correlation coefficient,  $R^2$ , of 0.9761 compared to the Langmuir isotherm. This implies that the adsorption isotherm data are well fitted by the Freundlich isotherm [29]. Hence, it can be concluded that the MB dye was adsorbed by the heterogenous surface EFB via multilayer biosorption. In order to support this statement, the adsorption intention ( $n$ ) was calculated and found to be 1.0366. Hence, it can be said that the adsorbent satisfied the condition of heterogeneity because its  $n$  value was between 1 and 10 ( $1 < n < 10$ ) [30].

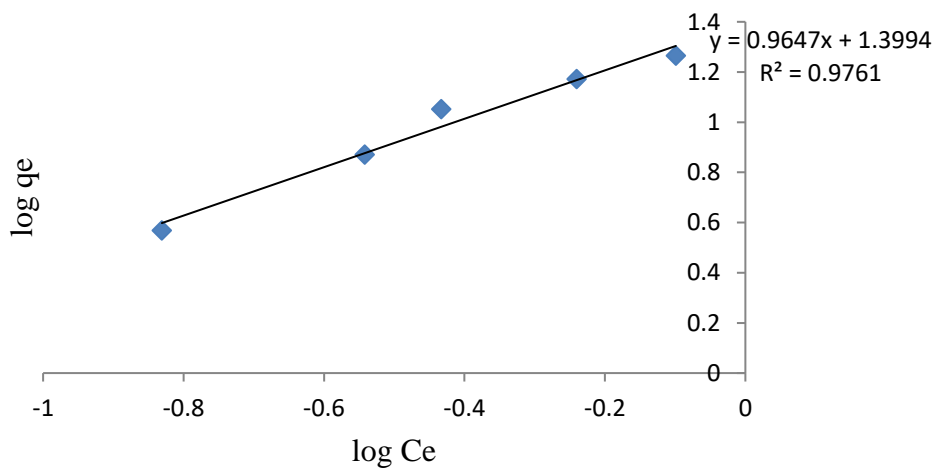


Figure 8. Freundlich isotherm.

**Table 3.** Langmuir and Freundlich isotherm constants

Langmuir isotherm				Freundlich isotherm		
$Q_o,$ mg/g	$K_L,$ L/g	$R_L$	$R^2$	$K_F$	$n$	$R^2$
151.5	0.1843	0.3517	0.1993	24.797	1.0366	0.9761

According to Rafeah *et al.* [25], when the percentage removal of adsorbate is low, it may be because the adsorbate was limited to only monolayer adsorption, which restricts the available sites on the adsorbent surface in which the dye can interact in order for adsorption to occur, and thus directly proves the Langmuir isotherm. However, the percentage removal of dye in this study was higher, hence, it does not suggest monolayer adsorption. Instead, it is more likely to be a multilayer adsorption process with a heterogenous surface EFB which supports the  $R^2$  value of the Freundlich isotherm. Table 3 summarizes the value of the constants for the Langmuir and Freundlich isotherms which were calculated from the linear isotherm graphs.

**Adsorption Kinetics Studies**

The kinetic data was then fitted into two models: a pseudo-first order kinetic model and a pseudo-second order kinetic model. The pseudo-first order kinetic model is widely used to predict adsorption kinetics and is defined as:

$$\log (q_e - q_t) = \log q_e - \frac{k_1 t}{2.303} \tag{6}$$

where  $q_e$  and  $q_t$  (mg/g) are the amounts of adsorbate adsorbed at equilibrium and at any given time,  $t$  (min) respectively, and  $k_1$  ( $\text{min}^{-1}$ ) is the adsorption rate constant. In order to determine the suitability of the experimental data, a graph of  $\log (q_e - q_t)$  versus  $t$  was plotted as shown in Figure 9.

The pseudo-second order equation predicts the behaviour over the whole adsorption process and is expressed as:

$$\frac{t}{q_t} = \frac{1}{k_2 q_e^2} + \frac{t}{q_e} \tag{7}$$

where  $k_2$  ( $\text{g mg}^{-1} \text{min}^{-1}$ ) is the rate constant of the pseudo-second order adsorption. In order to determine the suitability of the experimental data, a graph of  $\frac{t}{q_t}$  versus  $t$  was plotted as shown in Figure 10. The best fit model was selected based on the linear regression correlation coefficient ( $R^2$ ) values obtained from the linear pseudo-first order and pseudo-second order graphs.

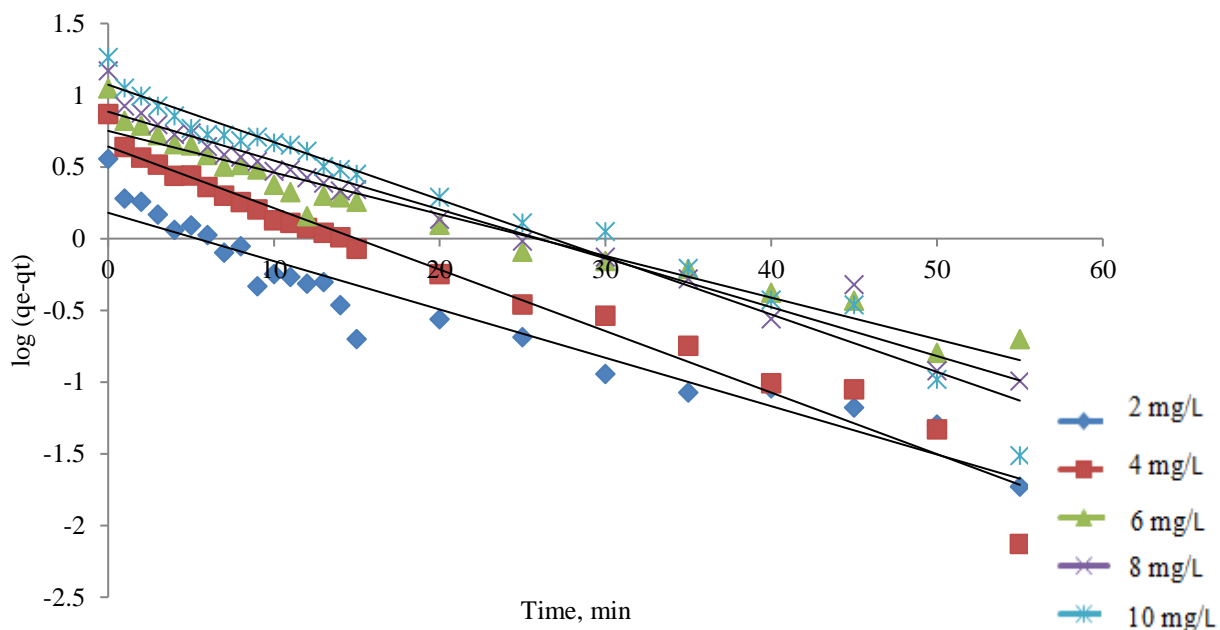


**Figure 9.** Pseudo-first order kinetic model graph for the adsorption of MB dye onto EFB biosorbent.

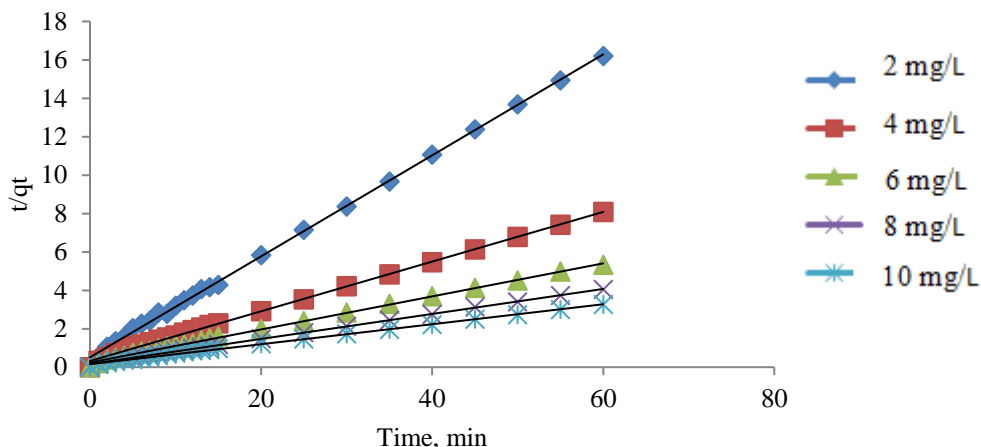


**Figure 10.** Pseudo-second order kinetic model graph for MB dye adsorption onto EFB biosorbent.

By comparing the results, the pseudo-second order model was selected as the best fit as its correlation coefficient,  $R^2$  was higher than that of the pseudo-first order model. This confirms the suitability of the pseudo-second order rate equation. Although the correlation coefficient of the pseudo-first order model was higher than 0.90, the experimental  $q_e$  values did not agree with the calculated value obtained from the linear plot [22]. Hence, it implies that the adsorption of MB onto EFB is not a pseudo-first order kinetic reaction. The comparison of experimental and calculated  $q_e$  values and the constants for the pseudo-first order and pseudo-second order models can be seen in Table 4.

### CONCLUSION

This study proves that EFB was able to remove MB from wastewater by biosorption. The removal of MB by EFB was influenced by the initial concentration of MB, contact time, pH, and biosorbent dosage. Maximum adsorption was found at pH 11 due to

negatively charged ions on the surface of EFB. This created a strong electrostatic attraction between EFB and cationic dyes which increased the adsorption capacity. The removal of MB increased with biosorbent dosage and decreasing MB concentration. Within the first 20 min, the removal rate of MB was observed to increase rapidly and equilibrium was attained within 60 min of contact time. Using FTIR spectroscopy, it was found that  $-OH$ ,  $C\equiv C$ ,  $C-O$ ,  $C-H$  stretching and  $N-H$  bending vibrations were present and involved in the adsorption process, while BET described EFB as a mesoporous material. The kinetic data obtained in this study fit well with the pseudo-second order model and the equilibrium data was consistent with the Freundlich isotherm which gave a high correlation coefficient of 0.9761. The Freundlich isotherm satisfied the EFB surface heterogeneity. Hence, the MB biosorption process was a multilayer adsorption interaction with the EFB surface. Based on this study, EFB showed good potential in removing MB from aqueous solution.

**Table 4.** Data for adsorption rate constants, adsorption capacity and correlation coefficients of pseudo-first order and pseudo-second order models using different initial concentrations of MB adsorbed by EFB.

Initial concentration, mg/L	Experimental $q_e$ , mg/g	Pseudo-first order			Pseudo-second order		
		Calculated $q_e$ , mg/g	$k_1$ , $\text{min}^{-1}$	$R^2$	Calculated $q_e$ , mg/g	$k_2$ , g/mg/min	$R^2$
2	3.7048	1.5142	0.0776	0.9276	3.8037	0.1351	0.9990
4	7.4259	4.3833	0.0988	0.9686	7.7339	0.0516	0.9988
6	11.2617	5.6389	0.0670	0.9500	11.6279	0.0302	0.9981
8	14.8499	7.6700	0.0785	0.9662	15.3609	0.0253	0.9985
10	18.4075	11.9674	0.0921	0.9652	19.2307	0.0174	0.9978

**Abbreviation list**

AC	Activated carbon
MB	Methylene blue
EFB	Empty fruit bunch
BET	Brunauer-Emmett-Teller
FTIR	Fourier transform infrared
UV-Vis	Ultraviolet-visible
IUPAC	International Union of Pure and Applied Chemistry

**ACKNOWLEDGEMENTS**

This research was supported by the Research Management Center of Universiti Malaya in collaboration with the Center of Research and Innovation of Universiti Malaysia Sabah (Grant No. GL0111 or UM Project code: CG071-2013). These contributions are gratefully acknowledged.

**REFERENCES**

- Jodeh, S. and Amarah, J. (2016) Removal of methylene blue from industrial wastewater in Palestine using polysiloxane surface modified with bipyrazolic tripodal receptor. *Moroccan Journal of Chemistry*, **4(1)**, 140–156.
- Velusamy, S., Roy, A., Sundaram, S. and Kumar Mallick, T. (2021) A Review on heavy metal ions and containing dyes removal through graphene oxide-based adsorption strategies for textile wastewater treatment. *The Chemical Record*, **21(7)**, 1570–1610.
- Bożęcka, A., Orlof-Naturalna, M. and Kopeć, M. (2021) Methods of Dyes Removal from Aqueous Environment. *Journal of Ecological Engineering*, **22(9)**, 111–118.
- Cengiz, S., Tanrikulu, F. and Aksu, S. (2012) An alternative source of adsorbent for the removal of dyes from textile waters: *Posidonia Oceanica* (L). *Journal of Chemical Engineering*, **189-190**, 32–40.
- Bakar, N. A., Othman, N., Yunus, Z. M., Zawawi, D., Norisman, N. S. and Hisham, M. H. (2020) Physico-chemical water quality parameters analysis on textile. *IOP Conf. Series: Earth and Environmental Science*, **498 (012077)**, 1-8.
- Hakim, H. M. A. and Supartono, W. (2021) Removal of methylene blue from water using sugar palm agro industry waste adsorbent. *IOP Conference Series: Earth and Environmental Science*, **667(012008)**, 1–9.
- Moussavi, G. and Khosravi, R. (2011) Removal of cationic dyes from aqueous solutions by adsorption onto pistachio hull waste. *Chemical Engineering Research and Design*, **89**, 2182–2189.
- Theydan, S. K. and Muthanna, J. A. (2012) Adsorption of methylene blue onto biomass-based activated carbon by FeCl<sub>3</sub> activation: equilibrium, kinetics & thermodynamic studies. *Journal of Analytical and Applied Pyrolysis*, **97**, 116–122.
- Aksu, Z., Erfugrul, S. and Donmez, G. (2010) Methylene blue biosorption by rhizopus arrhizus: Effect of sds (sodium dodecylsulfate) surfactant on biosorption properties. *Journal of Chemical Engineering*, **158**, 474–481.
- Rangabhashiyam, S., Anu, N. and Selvaraju, N. (2013) Sequestration of dye from textile industry wastewater using agricultural waste products as adsorbents. *Journal of Environmental Chemical Engineering*, **1(4)**, 629–641.
- Amran, M., Dalia, K. M., Wan Azlina, W. A. K. and Azni, I. (2011) Cationic and anionic dye adsorption by agricultural solid wastes: a comprehensive review. *Journal of Desalination*, **280**, 1–13.
- Anisuzzaman, S. M., Joseph, C. G., Krishnaiah, D., Bono, A. & Ooi, L. C. (2015) Parametric and adsorption kinetic studies of methylene blue removal from simulated textile water using durian (*Durio zibethinus murray*) skin. *Water Science and Technology*, **72(6)**, 896–907.
- Reddy, M. C. S., Sivaramakrishna, L. and Reddy, A. V. (2011) The use of agricultural waste material, jujuba seeds for the removal of anionic dye (congo red) from aqueous medium. *Journal of Hazardous Materials*, **203-204**, 118–127.
- Ghasemi, M., Naushad, M., Ghasemi, N. and Khosravi-fard, Y. (2013) Adsorption of Pb(II) from aqueous solution using new adsorbents prepared from agricultural waste: adsorption isotherm and kinetic studies. *Journal of industrial and Engineering Chemistry*, **20(4)**, 2193–2199.
- Shaiful, M. S., Chin, H. C., Sarani Zakaria and Poi, S. K. (2012) Cationic and anionic modification of oil palm empty fruit bunch fibers for the removal of dyes from aqueous solutions. *Journal of Bioresource Technology*, **128**, 571–577.

16. Rafatullah, M., Othman, S., Rokiah, H. and Anees, A. (2009) Adsorption of methylene blue on low-cost adsorbents. *Journal of Hazardous Materials*, **177**, 70–80.
17. Rebitanim, N. Z., Ghani, W. A. W. A. K., Mahmoud, D. K., Rebitanim, N. A. and Salleh, M. A. M (2012) Adsorption capacity of raw empty fruit bunch biomass onto methylene blue dye in aqueous solution. *Journal of Purity, Utility Reaction and Environment*, **1**, 45–60.
18. Nasir, N., Ahmad Zaini, M. A., Mohd-Setapar, S. and Hashim, H. (2015) Removal of methylene blue and copper (II) by oil palm empty fruit bunch sorbents. *Jurnal Teknologi*, **74**, 107–110.
19. Efiyanti, L., Indrawan, D. A., Hastuti, N. and Darmawan, S. (2020) The activated carbon produced from mayan bamboo (*Gigantochloa robusta* Kurz) and its application as dye removal. *IOP Conference Series: Materials Science and Engineering*, **935(012018)**, 1–9.
20. Aligizaki, K. K. (2005) Pore structure of cement-based material: testing, interpretation, and requirements, 1–11
21. Haris, M. R. H. M. and Sathasivam, K. (2009) The removal of methyl red from aqueous solution using modified using banana pseudostem fibres. *American Journal of Applied Science*, **6**, 1609–1700.
22. Hameed, B. H., Tan, I. A. W. and Ahmad, A. L. (2008) Adsorption Isotherm, Kinetic Modeling and Mechanism of 2,4,6-trichlorophenol on Coconut Husk- Based Activated Carbon. *Journal of Chemical Engineering*, **114**, 235–244.
23. Ponnusamy, S. K. and Subramaniam, R. (2013) process optimization studies of congo red dye adsorption onto cashew nut shell using response surface methodology. *International Journal of Industrial Chemistry*, **4**, 17.
24. Zhiqiang, Z., Siqing, X., Xuejiang, W., Aming, Y., Ling, C., Zhiliang, Z., Jianfu, Z., Nicole, J. R. and Didier, L. (2009) A novel biosorbent for dye removal: extracellular polymeric substance (eps) of proteus mirabilis. *Journal of Hazardous Material*, **163**, 279–284.
25. Rafeah, W., Zainab, N. and Veronica, U. J. (2009) Removal of mercury, lead, and copper from aqueous solution by activated carbon of palm oil empty fruit bunch. *Journal of World Applied Sciences*, **5**, 84–91.
26. Maximova, A. and Koumanova, A. (2008) Equilibrium and kinetics study of adsorption of basic dyes onto perofil from aqueous solutions. *Journal of the University of Chemical Technology and Metallurgy*, **43**, 101–108.
27. Krishna, G. B. and Arunima, S. (2003) Kinetics and thermodynamics of methylene blue adsorption on neem (*azadirachta indica*) leaf powder, *Dyes and Pigments*, **65**, 51–59.
28. Tan, I. A. W., Ahmad, A. L. & Hameed, B. H. (2007) Adsorption of basic dye on high surface-area activated carbon prepared from coconut husk: Equilibrium, kinetic and thermodynamic studies. *Journal of Hazardous Materials*, **154**, 337–346.
29. Azraa, A., Jain, K., Tong, K. S., Rozaini, C. A. and Tan, L. S. (2012) Equilibrium, kinetic, and thermodynamic studies on the adsorption of direct dye onto a novel green adsorbent developed from uncaria gambir extract. *Journal of Physical Science*, **23**, 1–13
30. Uddin, M. T., Rahman, M. A., Rukanuzzaman, M. and Islam M. A. (2017) A potential low cost adsorbent for the removal of cationic dyes from aqueous solutions. *Applied Water Science*, **7**, 2831–2842.